Article

Sustainable Proposal for Plant-Based Cementitious Composites, Evaluation of Their Mechanical, Durability and Comfort Properties

César A. Juárez-Alvarado [1], **Camille Magniont** [2], **Gilles Escadeillas** [2], **Bernardo T. Terán-Torres** [1], **Felipe Rosas-Diaz** [1] **and Pedro L. Valdez-Tamez** [1,*]

1   Facultad de Ingeniería Civil, Universidad Autónoma de Nuevo León, C. Pedro de Alba s/n, San Nicolás de los Garza 66455, NL, Mexico
2   LMDC, Université de Toulouse, INSAT, UPS, 31077 Toulouse, France
*   Correspondence: pedro.valdeztz@uanl.edu.mx

Abstract: This research evaluates four sustainable cementitious composites with sustainable plant fibers and bio-aggregates: (1) cementitious matrix composite with lechuguilla fibers (LFC) and (2) with flax fibers (FFC); and (3) cementitious matrix composite with wood shavings (WSC) and (4) with hemp shavings (HSC). The fibers are for reinforcement and the shavings act as bio-aggregates as a total replacement for limestone aggregates. The lechuguilla (LF) and flax (FF) fibers were treated; wood (WS) and hemp (HS) bio-aggregates were also processed. Nineteen mixtures were manufactured, and five were used as controls, and the hygrothermal, mechanical, and durability properties were evaluated. The results for LFC and FFC showed that fiber treatment negatively affected flexural–compressive strength; untreated LFC with accelerated deterioration had better mechanical behavior, higher density, and lower porosity than FFC. Strength and density decreased, but porosity increased with increasing fiber volume (Vf). Regarding WSC and HSC, the microstructure of WS and HS had a significant effect on the physical and mechanical properties. The high porosity influenced the results obtained, since it decreased compressive strength and bulk density; however, thermal conductivity, hygroscopicity, and vapor resistance showed better behavior in most cases than the control specimens, i.e., without bio-aggregates.

Keywords: cementitious composite; sustainability; plant-based materials; hygroscopicity; durability; bio-aggregate

1. Introduction

The increase in the world's population has led to the construction of larger and more expensive infrastructures that are designed for a specific minimum duration. The world population was 7942 million in 2022 according to the report of the United Nations Department of Economic and Social Affairs, and population growth is expected to continue increasing over time, mainly in cities in Africa, Asia, and Latin America, with projected growth reaching 9.7 billion in 2050 [1]. The need for affordable and sustainable housing is an inherently global problem, and numerous challenges remain in producing environmentally friendly construction products [2].

The rising problem of resource depletion and global pollution has challenged many researchers to look for new materials based on renewable resources. The construction sector struggles with four main environmental impacts: greenhouse gas emissions; energy consumption; natural resource consumption; and waste production. The alternative technologies currently adopted in buildings will have immediate consequences concerning energy consumption and emission patterns [3]. The consideration and application of sustainability practices in construction can generate a 35% reduction in CO_2 emissions, and water and energy consumption savings of 30% to 50%, respectively, and a reduction in solid waste disposal costs of up to 90% [4–7].

In this context, the concept of "sustainable construction" has been used to characterize construction that includes environmental criteria in the project conception, in the form of construction and maintenance, and, when the time comes, demolition of the infrastructure [8]. Most products came from renewable resources until the beginning of the 20th century; however, the enormous growth of the petrochemical industry slowed down the growth of biotechnological products [9]. The combination of plant materials with non-organic matrices to produce competitive composite materials is increasingly gaining attention based on the strategy of preventing the clearing of agroforestry resources as well as producing good economic returns for their cultivation, resulting in valuable benefits for the environment, favoring a comfortable habitat (humidity, thermal, and acoustic management) [10–12].

The agroindustry is a sector that mainly serves agriculture to meet the demand for food supplies. The unit operations implemented in the production chain of any raw material bring environmental problems, namely, the high production of associated residues [13]. An analysis of the use given to the residues obtained from different agro-industrial sectors shows, for instance, that the brewing industry uses 8% of the grain nutrients, while in the palm oil and cellulose industries, less than 9% and 30% are used, respectively, and in the coffee industry, only 9.5% of the weight of the fresh fruit is used for the preparation of the beverage, leaving 90.5% as residue [14]. Depending on the type of raw material, it can be treated to reduce the negative environmental impacts and to transform it into valuable products that can be used as raw materials for other production processes and generate additional economic income. Thus, one of the challenges of research in this area is to optimize the results and diversify the use of these raw materials. Hence, achieving greater waste utilization depends on creating a strong value proposition throughout the value chain [15]

The main environmental benefit of bio-based building materials is their carbon storage capacity, which could contribute to climate change limitations. For instance, the use of these by-products can bring enormous benefits to reducing the cost of most of the world's industries, such as biotechnology or construction, among others [13]. The widespread use of plant materials and their products is attributed to properties such as low density, high electrical resistance, specific modulus and stiffness, non-abrasive properties, and biodegradability, among others. On the other hand, plant materials are raw materials from renewable sources and are of high availability, although to use them correctly it is necessary to know their properties and limitations in more detail to include them in new projects. The use of these materials has allowed for the availability of cheap, biodegradable, and recyclable construction materials from renewable resources, and under certain conditions of preparation, the insulating effect is comparable to that of other synthetic materials widely used in the industry, such as polystyrene, but with greater variability in their mechanical properties, which allow diverse applications given the difficulty to recycle the material of synthetic origin [16]. Natural fibers and their use in construction materials will have a positive impact on the construction projects in which they are used, generating a reduction in greenhouse gas emissions, climate control energy savings (operational energy), and less waste generation [11,17]. On the other hand, the main disadvantage of using plant fibers is the durability of these fibers in the cement matrix and the compatibility between the two phases. Alkaline media tend to mineralize the fibers, which is associated with long-term loss of toughness of the composite material attributed to interfacial damage caused by the continuous volume change of the porous plant fibers in the cement matrix. In addition, the fibers in contact with the reaction water release water-soluble substances that interfere with the hydration of the cementitious material, decreasing its potential toughness [18].

The present research study proposes to evaluate sustainable plant-based cementitious composites: (1) a composite based on a cementitious matrix with natural lechuguilla fibers (LFC) and flax fibers (FFC) as reinforcement; and (2) a cementitious matrix composite with wood shavings (WSC) and hemp shavings (HSC) as bio-aggregates, and whose hygrothermal, mechanical, and durability properties were evaluated. The results are

expected to have an important benefit for the environment, for a comfortable habitat (improvements in the hygrothermal performance of the home), and as sustainable materials for dignified housing.

2. Materials and Mixtures

2.1. Cementitious Materials

Two types of Portland cement were used, namely, type III from México, which complies with ASTM C150-21 [19], and type II from France, which complies with UNE-EN 197-1 [20], with a relative density of 3.1 and 3.0, respectively. The fly ash used was class F according to ASTM C-618-19 [21], which was obtained from a thermoelectric power plant in the city of Nava, Coahuila, and its relative density was 2.2. In addition, a metakaolin was used, since this type of pozzolan is very reactive in hydraulic cementitious matrices, and it had a relative density of 2.5. The fly ash came from Mexico and the metakaolin came from France, and both pozzolans were used additionally. The chemical compositions of the cementitious substances are shown in Table 1.

Table 1. Chemical composition of cementitious materials.

Material	Chemical Composition (%)					
	SiO_2	Al_2O_3	Fe_2O_3	CaO	MgO	Na_2O
Cement Type III	14.99	4.26	3.15	68.11	1.23	0.37
Cement Type II	15.20	3.82	2.12	59.90	-	-
Fly ash	59.95	25.98	4.92	2.66	0.12	-
Metakaolin	65.90	25.10	4.26	1.63	0.10	-

2.2. Aggregates

Two types of fine aggregates were used, namely, crushed limestone sand (Mexico) and river sand (France). The physical properties of the aggregates are shown in Table 2, and their grain size is presented in Figure 1. The limestone aggregate complied with ASTM C33-18 [22], and the river aggregate complied with NF P18-545 [23]. The grain size of the aggregates improves the workability of the mixture when plant components are added. Previous studies have shown that particle sizes with a maximum size of less than 10 mm are adequate when organic materials are used in a cementitious matrix, since they allow for a uniform distribution and reduce the agglomeration effect of the aggregates [24].

Table 2. Physical properties of aggregates.

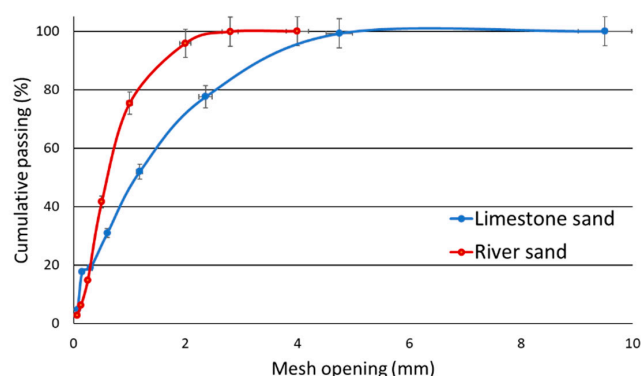|	Bulk Density kg/m³	Dry Weight kg/m³	Surface Dry Saturated Weight kg/m³	Water Absorption %	Specific Weight kg/m³	Water Content %	Fineness Modulus
Limestone	1651	2600	2617	1.60	2600	0.10	2.71
River	1660	2628	2660	1.54	2660	0.15	2.70

Figure 1. Particle grain size classification of aggregates.

2.3. Organic Materials

Two plant fibers were used as reinforcements; the first was the lechuguilla fiber (*Agave lechuguilla*) coming from the arid zones of Mexico, and the second was the flax fiber (*Linum*) from the south of France. Table 3 shows the physical and mechanical properties of the fibers. Pine wood shavings and commercial hemp shavings were used as bio-aggregates, and their properties are also shown in Table 3.

Table 3. Properties of organic materials [24–26].

| Material | Diameter/Width mm | Average Length mm | Physical and Mechanical Properties | | | | |
			Absorption %	Specific Weight	Tensile Strength MPa	Elongation %	Porosity %
Lechuguilla	0.16–0.26	45	92.3	1.38	275–627	2.0–2.5	21–25
Flax	0.009–0.049	45	120.0	1.54	1015	1.8–2.0	3–21
Wood	1.0	4.1	180.0	1.05	710	2.0–3.0	56
Hemp	1.8	7.6	105.0	1.50	900	1.6–1.8	51

2.4. Composition of the Mixtures

To choose the composition of the mix, one was looked for that met adequate workability and compaction parameters, which would allow for a better distribution and prevent agglomeration of the fibers and bio-aggregates in the mixture. Control mixes were produced to optimize the concrete proportions; a w/c ratio = 0.5 was used for the composites with fibers, and a w/c ratio = 1.0 for the composites with bio-aggregates. The mixtures with different formulations of both plant fibers and bio-aggregates are shown in Table 4. Table 5 shows the proportions of the five definitive control mixtures; their consistency was measured with the ASTM C143-20 slump test [27].

Table 4. Formulations of the mixes for the plant-based cementitious composites, % in volume.

Mixture	Composite	LF	FF	WS	HS	MK	FA
M1		0.4				15	
M2	LFC	0.7				15	
M3		1.0				15	
M4			0.4			15	
M5	FFC		0.7			15	
M6			1.0			15	
M7				2.0			
M8				4.0			
M9	WSC			2.0			20
M10				4.0			20
M11				10.0			20
M12					4.0		
M13	HSC				4.0	20	
M14					10.0	20	

Table 5. Proportion of the control composite mixture.

| Mixture | Mix Proportion (LFC–FFC) (kg/m^3) | | | | | |
	Type II Cement	Water	River Sand	Metakaolin	W/C Ratio	Slump (mm)
C-1	383	169	1350	68	0.50	50

| Mixture | Mix Proportion (WSC) (kg/m^3) | | | | | |
	Type III Cement	Water	Limestone Sand	Fly Ash	W/C Ratio	Slump (mm)
C-2	150	150	1928	0	1.00	72
C-3	150	150	1893	30 (20%)	1.00	75

| Mixture | Mix Proportion (HSC) (kg/m^3) | | | | | |
	Type II Cement	Water	River Sand	Metakaolin	W/C Ratio	Slump (mm)
C-4	150	150	1973	0	1.00	70
C-5	150	150	1941	30 (20%)	1.00	73

3. Experimental Procedure

3.1. Testing of LFC and FFC Specimens

A deterioration procedure was performed to study the durability of specimens fabricated with the M1–M6 mixtures corresponding to the LFC and FFC, with Vf values of 0.4%, 0.7%, and 1.0%. This accelerated deterioration procedure consisted of 8 wetting and drying (AD) cycles; in each cycle, the composites were exposed to one day of wetting and 3 days of drying, and the specimens without fibers that were exposed to this procedure were the control specimens. The fibers were treated (TF) with a wax-based coating (Emulwax 3060) for protection in the alkaline cementitious environment. Uncoated fibers were also used as controls (UF), and for all mixtures the fiber length was 45 mm. The experimentation of the LFC and FFC is described below.

To evaluate the flexural strength, three $40 \times 40 \times 160$ mm bars were fabricated for each test mixture. The specimens were demolded 24 h after fabrication, and during this period, water evaporation was prevented by protecting them with a plastic film, and they were kept at a room temperature of 20 °C. After specimens were extracted, they were kept for one week in a curing room at 20 °C with 100% relative humidity. Both fabrication and curing were performed using the procedure indicated in NF EN 196-1 [28]. The flexural strength of all specimens was evaluated at 40 days of age at the end of 8 exposure cycles according to NF EN 196-1 [28]. The compressive strength was obtained from the three specimens previously tested in flexure according to NF EN 196-1 [28]. Before testing, the specimens were dried in an oven at a temperature of 50 °C for 7 days to ensure that the specimens were completely dry.

Porosity and density are physical properties that are correlated and that have an impact on the durability of the material. The three samples from the specimens previously tested in compression were obtained, and their values were determined as described in NF P18-459 [29]. Finally, the interaction mechanisms of the fiber/matrix interface were determined by scanning electron microscopy. The observations were performed with a scanning electron microscope (JEOL JSM-6380LV). In order to limit the deterioration of the plant material, the observations were performed without coating the sample and at a vacuum of 60 Pa (LV) with an accelerating voltage of 15 kV.

3.2. Testing of WSC and HSC Specimens

Consumption values of 2%, 4%, and 10% substitution by volume of the aggregate were proposed, according to the method of absolute volumes. The following tests were carried out to evaluate the physical and mechanical behavior of these composites based on wood and hemp shavings.

To determine the compressive strength, 6 cylindrical specimens of 100×200 mm each were fabricated for each test formulation based on the specifications of ASTM C192-19 [30]. After 24 h of initial curing, all specimens were placed in the curing and maturing room at a temperature of $23° \pm 2$ °C at a relative humidity above 95% based on the recommendations of ASTM C511-21 [31]. Compression tests were performed at the corresponding ages according to ASTM C39-18 [32].

The bulk density was obtained in the 6 cylindrical and 3 prismatic specimens from the compressive strength and thermal conductivity tests, respectively. This was done by placing the specimens inside an oven at a temperature of $105° \pm 5$ °C in order to obtain a constant weight, which was related to the volume of each specimen, and thus the bulk density was obtained.

To measure the thermal conductivity, three prismatic specimens of $50 \times 150 \times 150$ mm each were manufactured for each test mixture according to the specifications of the Lambda Meter-500 equipment, intended for the hot plate method test according to RILEM recommendations in the RILEM-13 report [33]. The conductivity tests were performed according to the specifications of the measuring equipment and standards specified in the manual [34].

The MBV test consists of subjecting a specimen to cycles of high and low relative humidity to determine the humidity content that the composite material absorbs and

releases under these conditions. Three 50 × 150 × 150 mm prismatic specimens were prepared for each mixture. This test was performed in a climatic chamber at a preset temperature and relative humidity for a defined time. All specimens completed more than 20 cycles, which in total was more than 480 h of testing. The test was based on the research work "Moisture Buffering of Building Materials in Nordisk Innovations Center" [35].

For the measurement of water vapor permeability, two cylindrical specimens of 100 × 200 mm were produced, from which three slices of 100 × 25 mm were cut to be placed in metallic cups for the wet cup method. Additionally, two specimens of 110 × 220 mm were manufactured, from which three slices of 110 × 25 mm were cut to be placed in the metallic cups for the dry cup method. These tests were performed according to the specifications of NF EN ISO 12572:2001-10 [36].

The pore network of the WSC and HSC was analyzed by scanning electron microscopy, which allowed the complementing of the experimental results obtained for compressive strength, bulk density, heat transfer, moisture regulation in absorption and desorption cycles, and water vapor permeability. A scanning electron microscope (JEOL JSM-6380LV) was used.

4. Analysis and Discussion of the Results

4.1. Results of LFC and FFC Specimens

4.1.1. Flexural Strength

Figure 2 shows the results obtained for flexural strength at 40 days of age. The treatment of the fibers adversely affected the flexural strength for the LFC and FFC. In all cases, the untreated fibers showed better mechanical behavior; this was due to the better adhesion with the cementitious matrix without the presence of a wax-based coating [37]. Additionally, it is evident that this coating on the fibers did not provide adequate protection when the composites were exposed to accelerated deterioration. The LFC/TF resulted in lower flexural strength values than the 0% fiber volume, while the LFC/UF had an increase in flexural strength with respect to the 0% fiber volumes of 38%, 28%, and 16% for $V_f = 0.4\%$, 0.7%, and 1.0%, respectively. The FFC composites with and without coatings were more affected by accelerated deterioration for all fiber volumes exhibiting lower flexural strength than the control; this may have been due to flax fiber being more susceptible to degradation in alkaline environments. In all cases, a reduction in strength was observed as V_f increased [37].
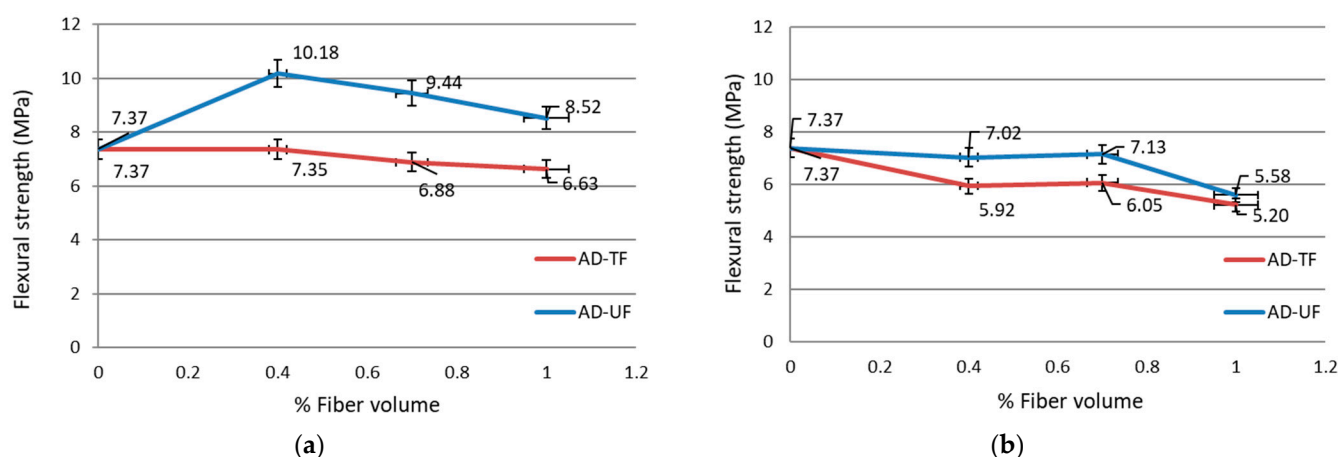

Figure 2. Flexural strength for different Vf values with exposure to accelerated deterioration. (**a**) LFC with and without fiber treatment. (**b**) FFC with and without fiber treatment.

4.1.2. Compressive Strength

Figure 3 shows the results of the compressive strength at 40 days of age. The behavior was similar to that of the flexural strength. The LFC composites with Vf = 0.4% without

wax coating had higher compressive strength than the control in 14%, and for all the Vf, the strengths were higher than those corresponding to the FFC, and the accelerated deterioration seemed to affect more the latter composites. The tendency for compressive strength to decrease with increasing Vf was maintained as in the bending behavior. The chemical composition of both LF and FF had an important role in their mechanical behavior, since by their nature they are mainly composed of cellulose, hemicellulose, and lignin, which provide strength, stability, and stiffness in the fiber [18] and can contribute to the mechanical properties of the developed composites. Their cellulose and lignin composition has an impact on the hydration process and finally on the development of flexural and compressive strength [38].
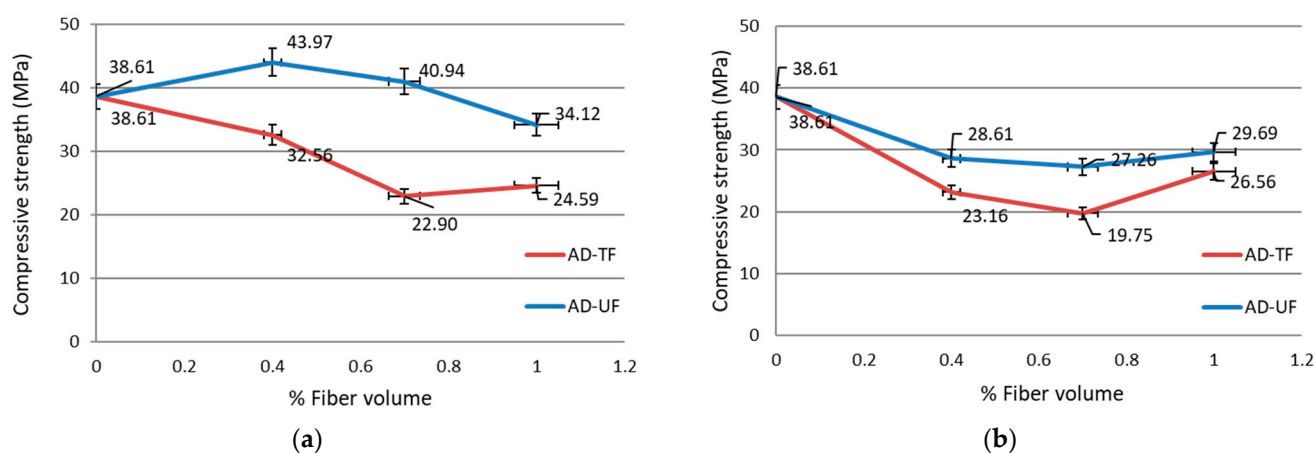

Figure 3. Compressive strength with exposure to accelerated deterioration. (**a**) LFC with and without fiber treatment. (**b**) FFC with and without fiber treatment.

4.1.3. Porosity and Density

The open porosity of a material is the ratio between the volume of pores communicating to the exterior and its total volume expressed in percentage. Porosity and dry density are properties that are related to each other. Figure 4 shows that porosity increased while density decreased with the increase of fibers in the matrix [39]. For LFC (Figure 4a), the results showed a slight increase in porosity of 1%, 7%, and 9% for fiber volumes of 0.4, 0.7, and 1.0%, respectively; these results agree with Siddique [40]. Figure 4b for FFC shows higher porosity than LFC, which may be due to the physical properties of flax fiber that have a higher absorption capacity than agave fibers, and this could cause a higher porosity in the composite.
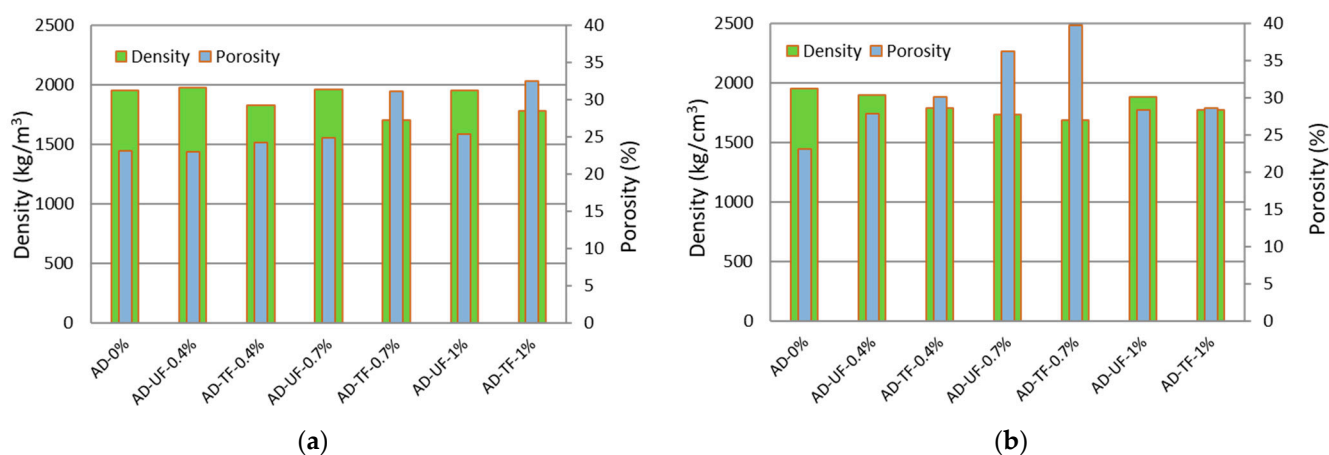

Figure 4. Relationship between porosity and density for specimens with exposure to accelerated deterioration. (**a**) LFC with and without fiber treatment. (**b**) FFC with and without fiber treatment.

Figure 4 shows that the treatment affects in a more significant manner the porosity/density than do the presence and the percentage of fibers in both composites. On the other hand, porosity and density are important properties of concrete, as they affect mechanical behavior. Figure 5 shows how compressive strength is affected by density and porosity, showing that the compressive strength increases with higher density and decreases with higher porosity [39]. The FFC showed lower density and higher porosity than LFC, which achieved higher compressive strength values.
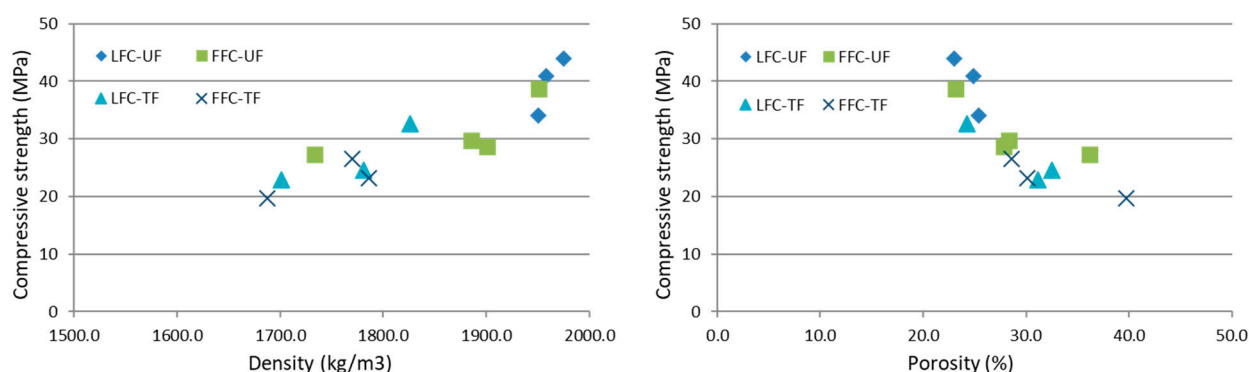

Figure 5. Effect of porosity and density on compressive strength at 40 days of age, for LFC–FFC specimens, with and without fiber treatment.

4.1.4. Microstructure of LFC and FFC with Deterioration

Figure 6 shows the micrographs of the LFC with accelerated deterioration. Deposits of mineral products on the fiber walls can be observed in Figure 6a,b, which were in the form of small plaques (white deposits), but these were not present in the depths of the fiber. This may be because matrix products could adhere to the fiber, but these did not embrittle the fiber, even in fibers without wax coatings. Figure 6c,d shows the failure mode of the fibers. In Figure 6c, the rupture of the untreated fiber caused by the adhesion to the cementitious matrix can be observed. While the treated fibers showed a pull-out type of failure due to adhesion failure, as can be seen in Figure 6d, it is clear that the adhesion between the LFs and the matrix is an important factor in the mechanical strength of the LFCs. The SEM observations show the interface with the cementitious matrix, where volumetric variations produced by water absorption could be observed because an amount of water absorbed by the fiber during mixing did not diffuse into the paste, and upon drying, it produced a reduction in volume. These dimensional variations could result in adhesion defects such as those observed in the micrographs (Figure 6d), which can lead to a loss of strength. Similar results of pull-out failures in FF have been reported in other studies [41].

Similarly, micrographs of the FFC with accelerated deterioration are shown in Figure 7. Figure 7b,d show that the flax fiber bundles did not disperse into individual fibers; this could have occurred when the fibers were incorporated into the mixture. The FF had a smaller diameter than the LF, which gave it more bonding surface area for the same volume; however, this was not evident in the mechanical results, as relatively good bonding between the FF and the matrix was lost due to the agglomeration of the FF. Additionally, in Figure 7a,b, some mineral deposits can be observed that are visible on the surface of the FF; after the accelerated deterioration procedure, the specimens were at least 60 days old at the time of the observations conducted, and with this elapsed time there were no signs of deep mineralization for the FF with and without treatment. This was evident by the fact that no embrittlement was observed in the fibers; on the contrary, they had a certain degree of ductility. SEM observations showed greater chemical interaction between the LFs with the mineral deposits compared to the FF, as they tended to have greater embrittlement, and their color changed. Other studies have used a metakaolin matrix as the formulation of this research, and they agree that this pozzolan can help to avoid the mineralization of plant fibers [42]. On the other hand, minimal volumetric variations of the untreated fiber

are observed in Figure 7c. The agglomeration shown in Figure 7d makes it evident that the flax fiber was not adequately distributed, which may have influenced the low flexural and compressive strength that the FFC showed. This also explains, however, the higher porosity of these composites.
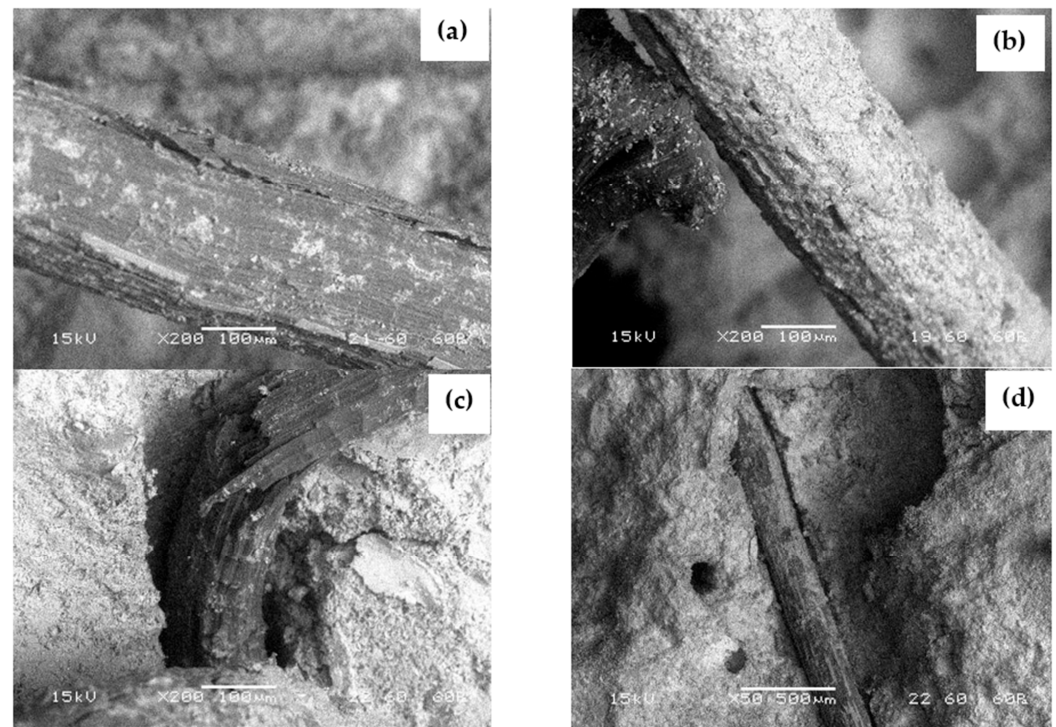

Figure 6. SEM observations: (**a**) (×200) untreated LFC; (**b**) (×200) treated LFC; (**c**) (×200) untreated LFC, failure mode rupture type; (**d**) (×50) treated LFC, failure mode pull-out type.
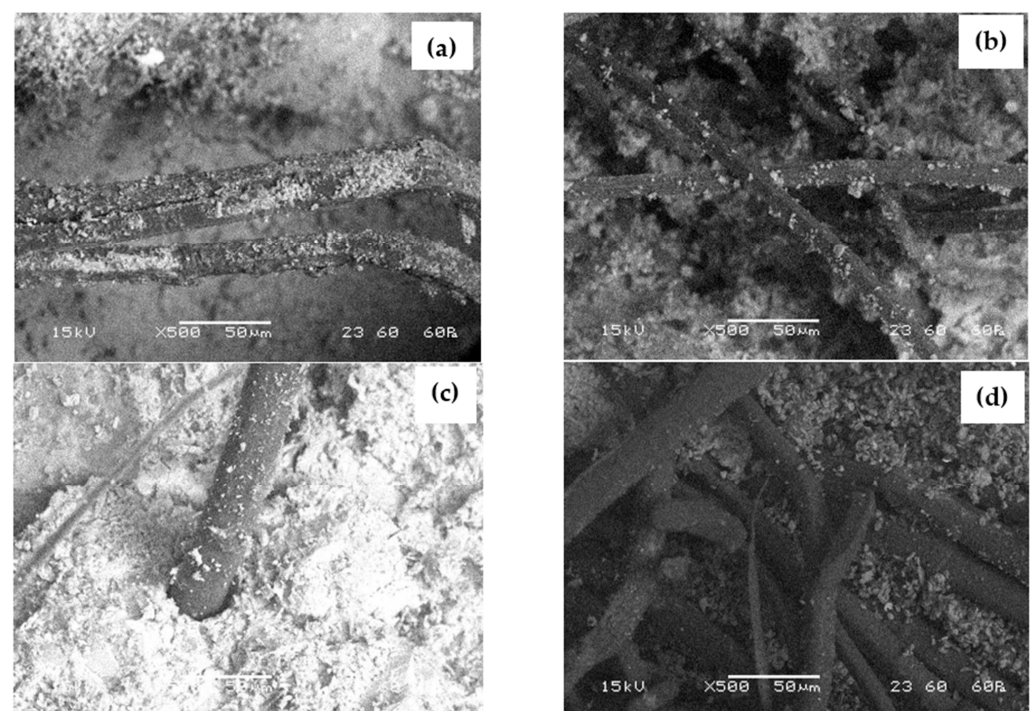

Figure 7. SEM observations (×500): (**a**) untreated FFC; (**b**) treated FFC; (**c**) untreated FFC, matrix–fiber interface; (**d**) treated FFC, matrix–fiber interface.

4.2. Results of WSC and HSC Specimens

4.2.1. Compressive Strength

The addition of porous plant aggregates led to a decrease in compressive strength, which was the expected behavior. The results of the compressive strength at 84 days of age of the composites are shown in Figure 8, where it is shown that the WSCs had better mechanical behavior than the HSCs. For WSC, the formulations M7 and M8 with 0% FA were similar to C2 (0% FA), but M9, M10, and M11 (20% FA) formulations did not exceed C3 (20% FA). Comparing C2 and C3, it was observed that the addition of FA produced a 59% increase in resistance; this contribution of FA had a positive impact on formulations M9 and M10. For HSC, the difference in resistance with respect to the control formulations C4 (0% MK) and C5 (20% MK) was not very significant; M12 (0% MK) was lesser than C4, and M13 and M14 with 20% MK were lesser than C5. In the case of HSC, it was mainly due to the presence of bio-aggregates (HS) with high water absorption capacity in the cementitious matrix, as well as the impact of hydrosolubility coming from HS on the hydration and hardening of the mineral matrix, which promoted a slower evolution in strength growth [43]. It was observed that both FA and MK behaved as fillers and also densified the matrix of WSC–HSC specimens.
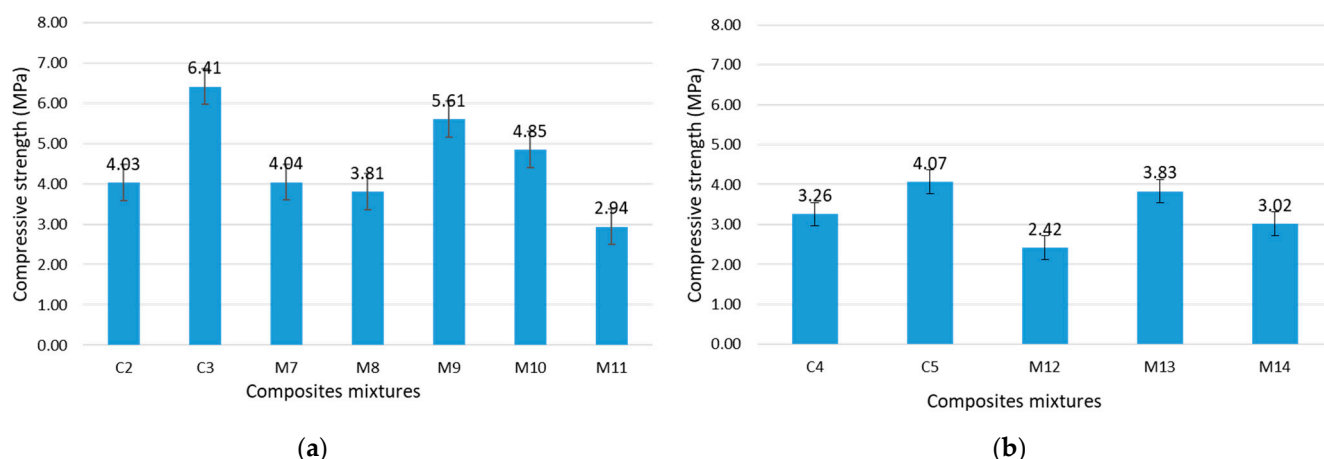

Figure 8. Variation of the compressive strength for the different formulations: (**a**) WSC, (**b**) HSC.

Figure 9 shows the effect of shavings replacement within the cementitious matrix; as the percentage of bio-aggregate replacement increased, there was a decrease in compressive strength. Figure 9a shows that for WSCs, for 10% WS replacement there was a 54% reduction with respect to the C3 control formulation with an FA-based matrix. HSC specimens with the MK matrix in contrast had a lower strength reduction of 26% for the maximum 10% replacement of HS compared to C5. It is evident that the presence of bio-aggregates affected the matrices with FA more than the matrices with MK and even the matrices that did not have cementitious agents, as can be seen in Figure 9b. However, the matrices with FA without bio-aggregates had a higher resistance to compression. A previous study found different mechanical behaviors, reporting that FA mortars had the lowest compressive strength values up to 180 days compared to MK mortars [44]. It is well known that if a sufficient amount of calcium hydroxide is not available in the early stages of cement hydration, the initial strength of the pozzolanic compounds forming additional calcium silicate may be lower than the strength of the control, which may explain the mechanical behavior observed in Figures 8 and 9.
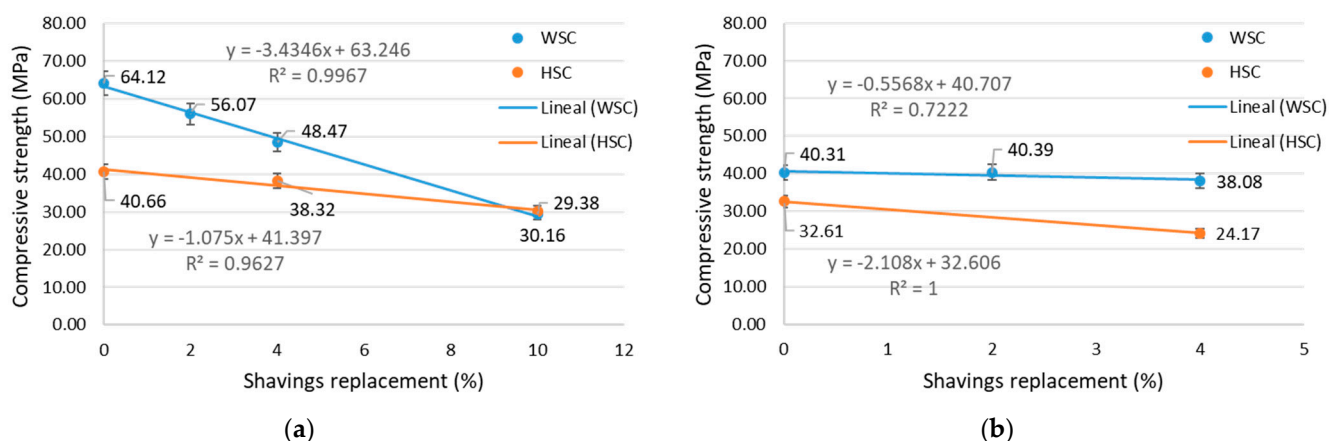
(a)

(b)

Figure 9. Effect of the shaving volume on the compressive strength for WSC–HSC specimens: (**a**) cementitious matrix with FA and MK; (**b**) cementitious matrix without FA and MK.

4.2.2. Density

The results of the bulk density are shown in Table 6. It was observed that all WSC formulations reduced their density with respect to the controls (0% WS) C2 and C3, with formulation M11 (10% WS) being the one that decreased up to 19% and 16%, respectively. The HSC had similar behavior; all formulations had lower densities than the C4 control (0% HS), and the formulation with higher shaving content of M14 (10% HS) decreased up to 13% with respect to the C4 control. With respect to the C5 control with 20% MK, the reduction was not very significant (2%), and even the formulations M12 and M13 had a slightly higher density, namely, 5% and 3%, respectively, with 4% HS. Higher percentages of WS and HS would be necessary to obtain even lower bulk density values; however, they must be related to the compressive strength in order not to affect its mechanical behavior.

Table 6. Variation of the bulk density for the different formulations (kg/m^3).

| Composite | Mixtures | | | | | | | | | | | |
	C-2	C-3	C-4	C-5	M7	M8	M9	M10	M11	M12	M13	M14
WSC	2121	2052			1786	1777	1775	1792	1728			
HSC			1900	1699						1788	1742	1658

Bulk density is affected by the accommodation of different shavings sizes within the cementitious matrix; thus, the pore content will have an impact on the reduction of bulk density in the specimens. The unit weight of the WSC and HSC decreased compared to the control specimens, as observed in Table 6. This reduction was also related to the fact that WS and HS were lighter than the fine aggregate, and this lightened the cementitious matrix [45]. Another aspect to consider is that during compaction, water is expelled from the shavings, leaving an unoccupied void within it, and subsequently these voids in the shavings are occupied by air [46]. The use of wood shavings has been found to substantially reduce the bulk density in cementitious composites and has comparable values with wood agglomerates [47].

4.2.3. Thermal Conductivity

The thermal behavior of the WSC and HSC are shown in Figure 10. It was observed that as the density decreased, the thermal conductivity also decreased. The highest density and the thermal conductivity of 0.7 W/(mK) were given by the control values, and all formulations produced lower results. As seen in Figure 10a, for the WSCs, the values showed that the use of WS decreased from 0.7 to 0.4 W/(mK), leading to a thermal conductivity decrease of approximately 43% with respect to the control, which is comparable to the materials classified as insulators [48]. As seen in Figure 10b, HSC specimens showed

a reduction in thermal conductivity from 0.7 to 0.4 W/(mK), which was lower than the control and which represents 31%, and its density was lower than WSCs. It is evident that for the same % of replacement, HSC is just as efficient as WSC in reducing the thermal conductivity, and the difference in the evolution of the thermal conductivity with respect to the shaving replacement, as shown in Figure 11, can also be attributed to the origin of the bio-aggregates, since the different morphological nature of the hemp for HSC and the wood used for the WSC affects the thermal conductivity.
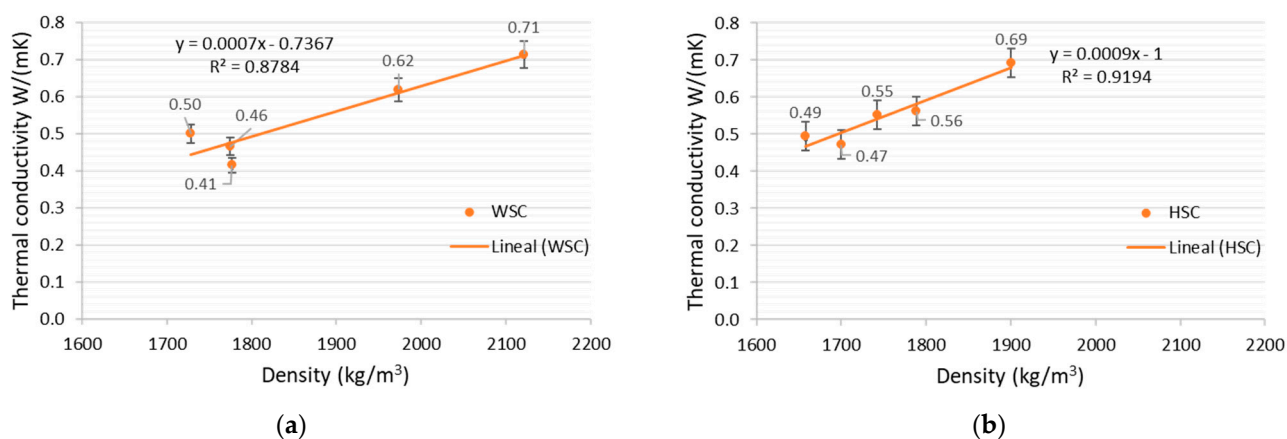

(**a**)   (**b**)

Figure 10. Effect of the bulk density with the thermal conductivity: (**a**) WSC, (**b**) HSC.
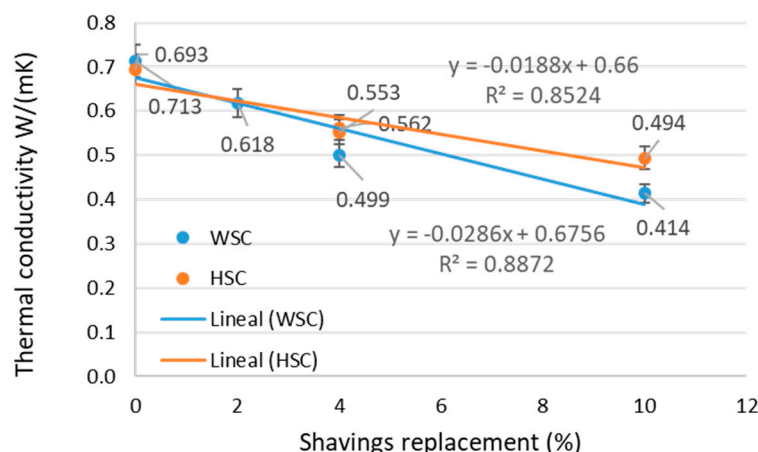

Figure 11. Effect of the shaving volume on the thermal conductivity for the WSC–HSC specimens.

As seen in Figure 11, increasing the content of shavings decreased the thermal conductivity of the composites and thus increased their insulating capacity. With the proportions of shavings used, the HSC showed slightly higher thermal conductivities than the WSC [49], and the tendency was to increase further with the increase of the replacement percentage. The low thermal conductivity of WSC was also related to the large number of voids, as reported in other studies [50]. The obtained values of thermal conductivity for WSC and HSC were relatively low and within the limits of lightweight and low thermal conductivity materials [50].

4.2.4. Moisture Buffering Value (MBV)

Figure 12 shows that the bulk density modified the MBV; as the density decreased, the MBV increased for WSC and HSC. Figure 12a shows that for WSC, the MBV values varied from 0.4 to 0.6 g/(m^2%RH), being higher for HSC, which varied from 0.8 to 1.0 g/(m^2%RH) (see Figure 12b). The control formulations were those with the highest density and lowest MBV, and it was observed that the presence of WS and HS led to an improvement in the

hygroscopic behavior by increasing the MBV, and the effect of HS was more evident. For the same density, HSC mixtures exhibited higher MBV than WSC; we can thus conclude that the nature of the cementitious matrix and the nature of the plant aggregate significantly affected the buffering behavior of the composite. The decrease in density was produced mainly by the porous structure of the WSC and HSC, which was primarily due to the nature of the bio-aggregates themselves and to the effect of the inclusion of these materials in a cementitious matrix. It is evident that porosity influenced the decrease in density and also the improvement of the hygroscopic behavior and water vapor permeability, as will be seen later [51].
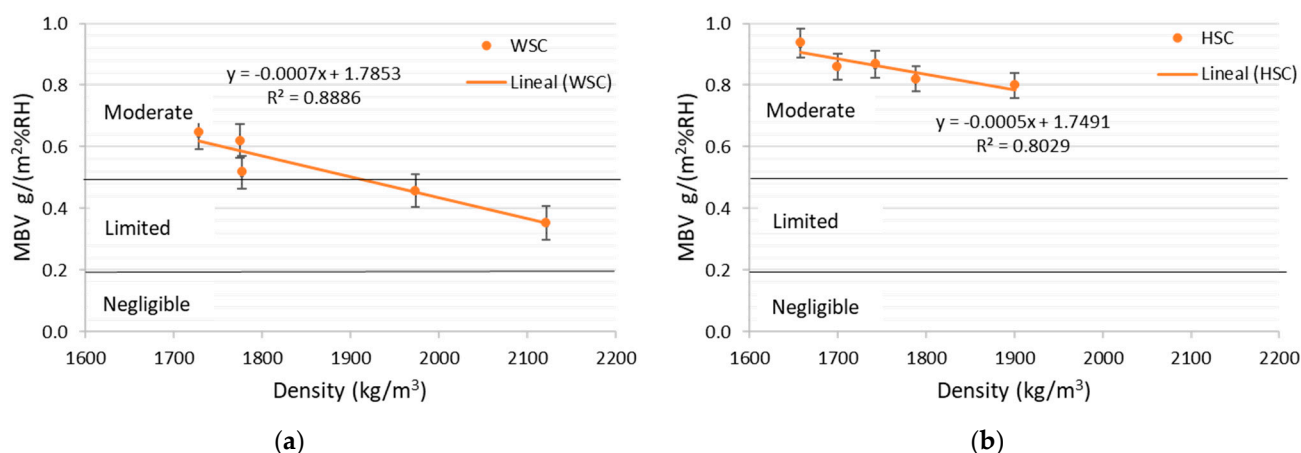

(**a**)   (**b**)

Figure 12. Effect of the bulk density with MBV: (**a**) WSC, (**b**) HSC.

Table 7 shows ranges of values for the MBV classification; according to these value, the WSC and HSC could be classified in the moderate category (0.5–1.0) for moisture regulation, which for a material with a cementitious matrix is adequate. The aforementioned can be seen in Figure 13, where the average MBV values are shown for different materials. For example, concrete and brick had a value of approximately 0.4 $g/(m^2\%RH)$, similar to the control formulation of WSCs. For HSCs with a higher percentage of HS (10%), the MBV values were approximate to the order of cellular concrete [35].

Table 7. Ranges for practical moisture buffer value classes [35].

MBV Practical Class	Minimum MBV Level	Maximum MBV Level
	$g/(m^2\%RH)$	
Negligible	0	0.2
Limited	0.2	0.5
Moderate	0.5	1.0
Good	1.0	2.0
Excellent	2.0	-

It is important to know the moisture-regulating properties of the materials to classify them in accordance with Table 7 and Figure 13; in this manner, one can have an idea of the behavior they will have in their specific application. Thus, a material with excellent conditions to regulate moisture will be able to absorb moisture and release it quickly. This will allow one to know if the WSC and HSC are able to regulate the humidity of the environment (absorption and desorption) to which they are exposed.
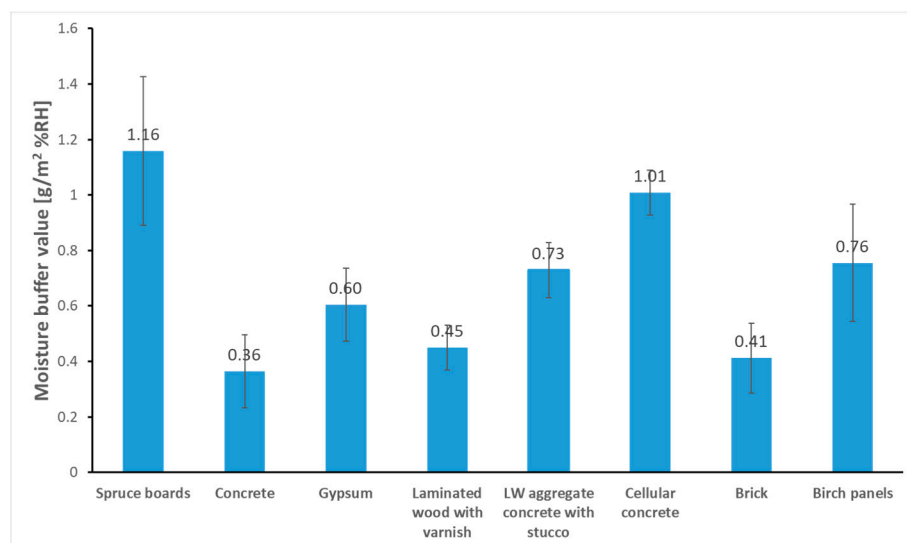
Figure 13. Average MBV values for different materials [35].

4.2.5. Water Vapor Permeability

Figure 14 shows the behavior of WSC and HSC with respect to the water vapor resistance factor. Figure 14a for WSC shows that the WS effect caused a reduction in the factor with respect to the C2 and C3 controls, allowing the transfer of moisture in greater quantities. Formulation M8 was the one that had a significant reduction with respect to the other formulations and the controls. Figure 14b shows that all the HSC formulations, including the controls, had higher water vapor permeability than those obtained for the WSCs. The HSCs were able to release more moisture to the environment due to the porous microstructure of HS, which caused an increase in the flow of water vapor passing through the capillary tubes, leading to higher moisture transfer. Other studies on hygroscopic materials have found that the presence of palm fibers in these composites decreases the resistance to water vapor diffusion and improves moisture transfer, and also in concretes with hemp there is a high permeability to water vapor, regardless of age [52]. These results can be positive depending on the place of application, since it can serve as a buffer to sudden changes in humidity; however, in cold places, it can affect the thermal performance of the envelope, and therefore it is a factor that should be considered at the time of application.
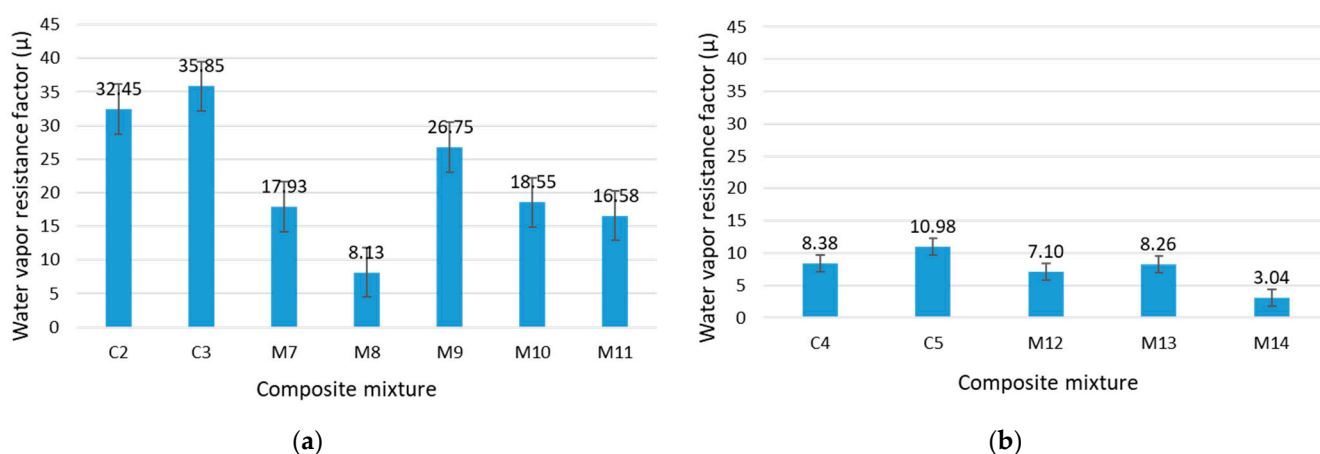

(**a**)

(**b**)

Figure 14. Variation of the water vapor permeability for different formulations: (**a**) WSC, (**b**) HSC.

4.2.6. Microstructures of WS and HS

Figure 15a,b show micrographs of WS, where high porosity can be observed from the micrographs. WS was found to be composed of 60% cellulose, and cellulose has a fibrous

structure originating from compact microfibrils that constitute the plant cell wall [53]. WS had a three-dimensional cellular microstructure, with an orientation of stiff cellulose microfibrils in a matrix of hemicellulose and lignin (see) Figure 15a,b. Hemicelluloses are closely associated with cellulose microfibrils, and these are embedded with lignin, which gives it its mechanical and physical properties [54]. HS, as can be observed in Figure 15c,d, had a distribution of cells or micropores with dimensions of 20–25 μm wide by 40–50 μm long in a tubular shape. Figure 15c shows a separation between the large parenchyma cells seen in the upper section and the lower part with smaller longitudinal parenchyma cells. In Figure 15d, the micropore walls that are not pitted can be seen. In other studies, it has been observed that some walls show cell-to-cell pitting [55]. HS is a highly porous material, as opposed to WS, as can be seen in the micrographs. HS has an approximate porosity 25 times larger than WS, due to the species type and stem size. The higher porosity of HS observed in its microstructure explains the lower compressive strength and bulk density, along with a better performance in thermal conductivity, moisture regulation in absorption and desorption cycles (MBV), and water vapor permeability, as shown in the experimental results of HSC.
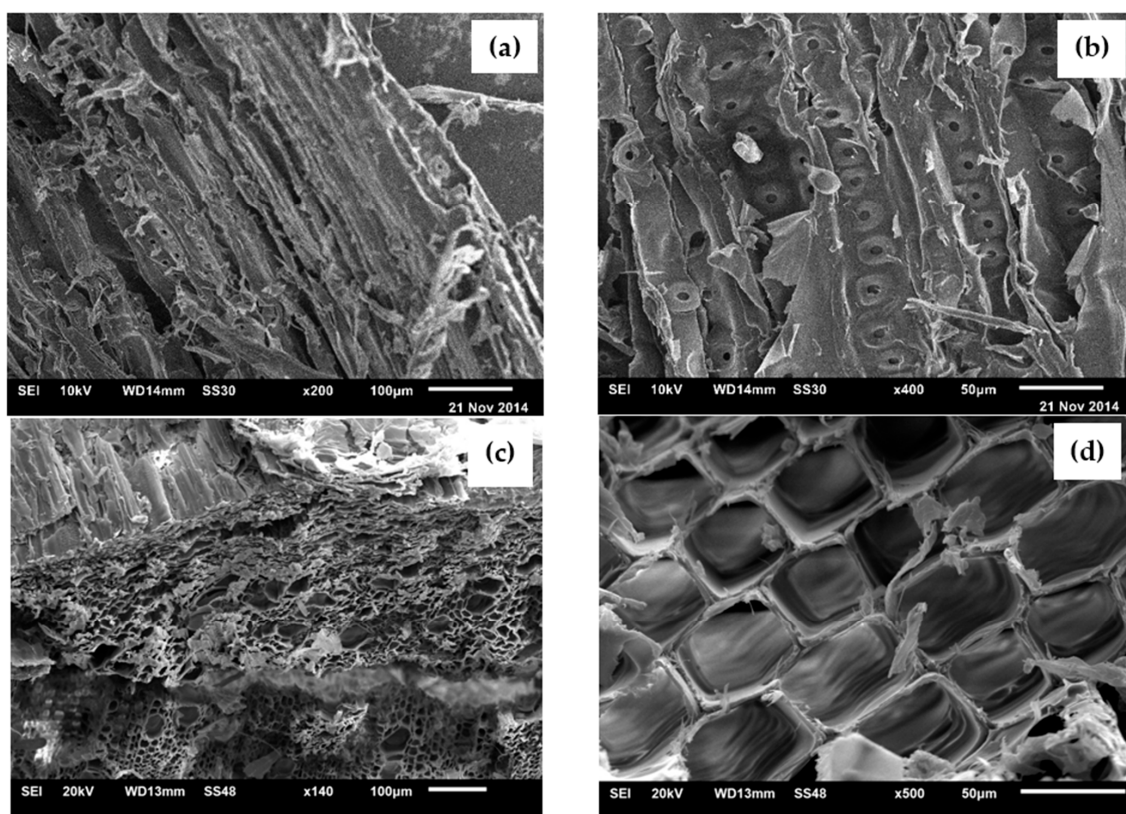

Figure 15. SEM observations of WS at (**a**) ×200 and (**b**) ×400, and HS at (**c**) ×140 and (**d**) ×500.

5. Conclusions

The present study aimed to determine the physical, mechanical, microstructural, and durability properties of sustainable plant-based concretes in order to reduce the environmental impact of conventional concretes, and the conclusions for each of the proposals are presented below:

(1) LFC and FFC with wax treatment on the fibers had an adverse effect on flexural strength; on the other hand, untreated fibers and those with accelerated deterioration showed better mechanical behavior, since they had an increase in flexural strength with respect to the control of 38% and 19%, respectively, for a Vf = 0.4%. Flexural and compressive strength decreased with increasing Vf. Although the fibers may not

improve the flexural strength still they contribute to reducing the brittleness of the material by allowing performance to be maintained after the first cracks appear.

(2) Porosity increases while density decreases when there is the presence of fibers in the matrix. The FFC presented higher porosity than LFC, which could be due to the higher porosity of the FF; in addition, the agglomeration shown in the micrographs is evidence that the FF does not have a uniform distribution within the matrix, and this could cause larger voids in the matrix, which influenced the low flexural and compressive strength shown by the FFC.

(3) Micrographs of LFC and FFC with accelerated deterioration showed no signs of fiber embrittlement in any case, even in the untreated fibers. The failure mode for the untreated LF was the rupture type and with treatment was the pull-out type, which explains the flexural and compressive behavior of the composites.

(4) The microstructure of WS and HS had a significant effect on all physical and mechanical properties of the composites. The high porosity influenced the experimental results obtained since it decreased the compressive strength and bulk density; however, for the thermal conductivity, hygroscopicity, and vapor resistance, it showed a behavior in most cases better than the controls that did not have bio-aggregates.

(5) The incorporation of WS and HS was important in improving the hygrothermal properties of the composites. On the other hand, WSC and HSC showed reductions in thermal conductivity values of 43% and 31%, respectively, with respect to the controls without bio-aggregates. These results are comparable with those established in the current regulations for low conductivity or insulating materials. The WSC and HSC are classified in the moderate category according to the MBV classification, and in comparison with values established for other materials with respect to the efficiency of moisture regulation, the HSC with the highest volume of bio-aggregate (10%); the MBV values are of the order of cellular concrete.

(6) Although the results demonstrate the positive effects of using vegetable raw materials as reinforcement or aggregate in cementitious matrices, future research should focus on the variability of the raw materials by incorporating local agricultural residues and on the long-term durability of the developed composites considering the incompatibility that may exist on the use of natural fibers in alkaline environments.

Author Contributions: Conceptualization, C.A.J.-A.; Formal analysis, C.M.; Investigation, C.A.J.-A.; Methodology, C.M. and G.E.; Validation, C.A.J.-A., C.M. and G.E.; Writing—original draft, C.A.J.-A., B.T.T.-T. and F.R.-D.; Writing—review and editing, C.M., G.E. and P.L.V.-T. All authors have read and agreed to the published version of the manuscript.

Institutional Review Board Statement: Not applicable.

Informed Consent Statement: Not applicable.

Data Availability Statement: Not applicable.

Conflicts of Interest: The authors declare no conflict of interest.

References

1. United Nations Department of Economic and Social Affairs, Population Division. *World Population Prospects 2022: Summary of Results*; United Nations Publication: New York, NY, USA, 2022.
2. Silva, F.D.A.; Mobasher, B.; Filho, R.T. Cracking mechanisms in durable sisal fiber reinforced cement composites. *Cem. Concr. Compos.* **2009**, *31*, 721–730. [CrossRef]
3. García, G.A. Energía en Edificaciones. *Rev. Mex. Física* **2013**, *59*, 44–51.
4. Agudelo, H.A.; Hernández, A.V.; Cardona, D.A.R. Sostenibilidad: Actualidad y necesidad en el sector de la construcción en Colombia. *Gestión Y Ambiente* **2012**, *15*, 105–118.
5. Masson-Delmotte, V.; Zhai, P.; Pirani, A.; Connors, S.L.; Péan, C.; Berger, S.; Caud, N.; Chen, Y.; Goldfarb, L.; Gomis, M.I.; et al. IPCC: Summary for Policymakers. In *Climate Change 2021: The Physical Science Basis. Contribution of Working Group I to the Sixth Assessment Report of the Intergovernmental Panel on Climate Change*; Cambridge University Press: Cambridge, UK, 2021; Volume 32.
6. Becchio, C.; Corgnati, S.P.; Kindinis, A.; Pagliolico, S. Improving environmental sustainability of concrete products: Investigation on MWC thermal and mechanical properties. *Energy Build* **2009**, *41*, 1127–1134. [CrossRef]
7. Rosas-Díaz, F.; García-Hernández, D.G.; Mendoza-Rangel, J.M.; Terán-Torres, B.T.; Galindo-Rodríguez, S.A.; Juárez-Alvarado, C.A. Development of a Portland Cement-Based Material with *Agave salmiana* Leaves Bioaggregate. *Materials* **2022**, *15*, 6000. [CrossRef] [PubMed]
8. Mora, E.P. Life cycle, sustainability and the transcendent quality of building materials. *Build. Environ.* **2007**, *42*, 1329–1334. [CrossRef]
9. Mohanty, A.K.; Misra, M.; Drzal, L.T.; Selke, S.E.; Harte, B.R.; Hinrichsen, G. *Natural Fibers, Biopolymers, and Biocomposites*; Taylor & Francis Group: Boca Raton, FL, USA, 2016. [CrossRef]
10. Krishna, N.K.; Prasanth, M.; Gowtham, R.; Karthic, S.; Mini, K.M. Enhancement of properties of concrete using natural fibers. *Mater. Today Proc.* **2018**, *5*, 23816–23823. [CrossRef]
11. Amziane, S.; Sonebi, M. Overview on Biobased Building Material made with plant aggregate. *RILEM Tech. Lett.* **2016**, *1*, 31. [CrossRef]
12. Mohammadkazemi, F.; Doosthoseini, K.; Ganjian, E.; Azin, M. Manufacturing of bacterial nano-cellulose reinforced fiber-cement composites. *Constr. Build. Mater.* **2015**, *101*, 958–964. [CrossRef]
13. Mythili, R.; Venkatachalam, P.; Subramanian, P.; Uma, D. Characterization of bioresidues for biooil production through pyrolysis. *Bioresour. Technol.* **2013**, *138*, 71–78. [CrossRef]
14. Cury R, K.; Aguas M, Y.; Martinez M, A.; Olivero V, R.; Chams Ch, L. Residuos agroindustriales su impacto, manejo y aprovechamiento. *Rev. Colomb. De Cienc. Anim.—RECIA* **2017**, *9*, 122. [CrossRef]
15. Mohanty, A.K.; Vivekanandhan, S.; Pin, J.-M.; Misra, M. Composites from renewable and sustainable resources: Challenges and innovations. *Science* **2018**, *362*, 536–542. [CrossRef]
16. Restrepo, S.M.V.; Arroyave, G.J.P.; Vásquez, D.H.G. Uso de Fibras Vegetales en Materiales Compuestos de Matriz Polimérica: Una Revisión Con Miras a SU Aplicación en El Diseño de Nuevos Productos Use of Vegetable Fibers in Polymer Matrix Composites: A Review. *Informador Técnico* **2016**, *80*, 77–86. [CrossRef]
17. Chabannes, M.; Nozahic, V.; Amziane, S. Design and multi-physical properties of a new insulating concrete using sunflower stem aggregates and eco-friendly binders. *Mater. Struct. Constr.* **2015**, *48*, 1815–1829. [CrossRef]
18. Sood, M.; Dwivedi, G. Effect of fiber treatment on flexural properties of natural fiber reinforced composites: A review. *Egypt. J. Pet.* **2018**, *27*, 775–783. [CrossRef]
19. *ASTM C150/C150M-2021*; Standard Specification for Portland Cement. American Society for Testing and Materials International: West Conshohocken, PA, USA, 2021; Volume I, pp. 1–10.
20. *UNE-EN 197-1*; Cemento. Parte 1. Composición, Especificaciones y Criterios de Conformidad de los Cementos Comunes. Asociación Española de Normalización y Certificación: Madrid, Spain, 2011; pp. 1–38.
21. *ASTM C-618-19*; Standard Specification for Coal Fly Ash and Raw or Calcined Natural Pozzolan for Use in Concrete. American Society for Testing and Materials International: West Conshohocken, PA, USA, 2019; pp. 1–4.
22. *ASTM C-33-18*; Standard Specification for Concrete Aggregates. American Society for Testing and Materials International: West Conshohocken, PA, USA, 2018; pp. 1–8.
23. *NF P18-545*; Granulats—Elément de Définition, Conformité et Codification, Normes Nationales et Documents Normatifs Nationaux. Association Française de Normalisation Editions: Paris, France, 2011; pp. 1–11.
24. *ACI Committe 544.1R-96*; State-of-the-Art Report on Fiber Reinforced Concrete. ACI Manual of Concrete Practice. American Concrete Institute: Farmington Hills, MI, USA, 1996; pp. 544.1R-1–544.1R-66.
25. Bederina, M.; Marmoret, L.; Mezreb, K.; Khenfer, M.; Bali, A.; Quéneudec, M. Effect of the addition of wood shavings on thermal conductivity of sand concretes: Experimental study and modelling. *Constr. Build. Mater.* **2007**, *21*, 662–668. [CrossRef]
26. Jiang, Y.; Ansell, M.P.; Jia, X.; Hussain, A.; Lawrence, M. Physical characterisation of hemp shiv: Cell wall structure and porosity. *Acad. J. Civ. Eng.* **2017**, *35*, 22–28.
27. *ASTM C143/C143M-20*; Standard Test Method for Slump of Hydraulic-Cement Concrete. American Society for Testing and Materials International: West Conshohocken, PA, USA, 2020; pp. 1–4.
28. *NF-EN 196-1*; Méthodes D'essais des Ciments—Partie 1: Détermination des Résistances Mécaniques. Normes Nationales et Documents Normatifs Nationaux. Association Française de Normalisation Editions: Paris, France, 2011; pp. 1–12.

29. *NF P 18-459*; Béton—Essai Pour Béton Durci—Essai de Porosité et de Masse Volumique. Normes Nationales et Documents Normatifs Nationaux. Association Française de Normalisation Editions: Paris, France, 2011; pp. 1–8.

30. *ASTM C192/C192M-19*; Standard Practice for Making and Curing Concrete Test Specimens in the Laboratory. American Society for Testing and Materials International: West Conshohocken, PA, USA, 2019; pp. 1–8.

31. *ASTM C511-21*; Standard Specification for Mixing Rooms, Moist Cabinets, Moist Rooms, and Water Storage Tanks Used in the Testing of Hydraulic Cements and Concretes. American Society for Testing and Materials International: West Conshohocken, PA, USA, 2021; pp. 1–3.

32. *ASTM C39/C39M-18*; Standard Test Method for Compressive Strength of Cylindrical Concrete Specimens. American Society for Testing and Materials International: West Conshohocken, PA, USA, 2018; pp. 1–7.

33. *RILEM-13*; Round Robin Test for Hemp Shiv Characterisation: Committee Report of tc—236 Bio-Based Building Materials. Springer: Berlin, Germany, 2013.

34. Dresden, L.-M.G. *Système de Mesure de Conductivité Thermique*; Université Paul Sabatier—Toulouse III: Toulouse, France, 2008.

35. Peuhkuri, R.H.; Mortensen, L.H.; Hansen, K.K.; Time, B.; Gustavsen, A.; Ojanen, T.; Ahonen, J.; Svennberg, K.; Arfvidsson, J.; Harderup, L.-E. *Moisture Buffering of Building Materials*; Rode, C., Ed.; BYG Report No. R-127; Technical University of Denmark, Department of Civil Engineering: Lyngby, Denmark, 2005; pp. 1–79.

36. *NF EN ISO 12572:2001-10*; Détermination des Propriétés de Transmission de la Vapeur D'eau. Norme Fracaise—European Norme: Association Française de Normalisation Editions: Paris, France, 2010; pp. 1–33.

37. Juarez, C.; Duran, A.; Valdez, P.; Fajardo, G. Performance of "*Agave lecheguilla*" natural fiber in portland cement composites exposed to severe environment conditions. *Build. Environ.* **2007**, *42*, 1151–1157. [CrossRef]

38. Kesikidou, F.; Stefanidou, M. Natural fiber-reinforced mortars. *J. Build. Eng.* **2019**, *25*, 100786. [CrossRef]

39. Lertwattanaruk, P.; Suntijitto, A. Properties of natural fiber cement materials containing coconut coir and oil palm fibers for residential building applications. *Constr. Build. Mater.* **2015**, *94*, 664–669. [CrossRef]

40. Siddique, R.; Klaus, J. Influence of metakaolín on the properties of mortar and concrete: A review. *Appl. Clay Sci.* **2009**, *43*, 342–400. [CrossRef]

41. Sabathier, V.; Magniont, C.; Escadeillas, G.; Juarez, C.A. Flax and hemp fibre reinforced pozzolanic matrix: Evaluation of impact of time and natural weathering. *Eur. J. Environ. Civ. Eng.* **2016**, *21*, 1403–1417. [CrossRef]

42. Melo Filho, J.D.A.; Silva, F.D.A.; Filho, R.T. Degradation kinetics and aging mechanisms on sisal fiber cement composite systems. *Cem. Concr. Compos.* **2013**, *40*, 30–39. [CrossRef]

43. Arnaud, L.; Gourlay, E. Experimental study of parameters influencing mechanical properties of hemp concretes. *Constr. Build. Mater.* **2012**, *28*, 50–56. [CrossRef]

44. Mardani-Aghabaglou, A.; Sezer, G.İ.; Ramyar, K. Comparison of fly ash, silica fume and metakaolin from mechanical properties and durability performance of mortar mixtures view point. *Constr. Build. Mater.* **2014**, *70*, 17–25. [CrossRef]

45. Li, Z.; Wang, X.; Wang, L. Properties of hemp fibre reinforced concrete composites. *Compos. Part A Appl. Sci. Manuf.* **2006**, *37*, 497–505. [CrossRef]

46. Mohammed, B.S.; Abdullahi, M.; Hoong, C.K. Statistical models for concrete containing wood chipping as partial replacement to fine aggregate. *Constr. Build. Mater.* **2014**, *55*, 13–19. [CrossRef]

47. Coatanlem, P.; Jauberthie, R.; Rendell, F. Lightweight wood chipping concrete durability. *Constr. Build. Mater.* **2006**, *20*, 776–781. [CrossRef]

48. *NMX-AA-164-SCFI-2013*; Edificación Sustentable: Criterios Y Requerimientos Ambientales Mínimos. Normas Mexicanas, Secretaría de Economía: Cd. de México, Mexico, 2013; pp. 1–158.

49. Uysal, H.; Demirbog, R. The effects of different cement dosages, slumps, and pumice aggregate ratios on the thermal conductivity and density of concrete. *Cem. Concr. Res.* **2004**, *34*, 845–848. [CrossRef]

50. Lagouin, M.; Magniont, C.; Sénéchal, P.; Moonen, P.; Aubert, J.-E.; Laborel-préneron, A. Influence of types of binder and plant aggregates on hygrothermal and mechanical properties of vegetal concretes. *Constr. Build. Mater.* **2019**, *222*, 852–871. [CrossRef]

51. Haba, B.; Agoudjil, B.; Boudenne, A.; Benzarti, K. Hygric properties and thermal conductivity of a new insulation material for building based on date palm concrete. *Constr. Build. Mater.* **2017**, *154*, 963–971. [CrossRef]

52. Bennai, F.; Issaadi, N.; Abahri, K.; Belarbi, R.; Tahakourt, A. Experimental characterization of thermal and hygric properties of hemp concrete with consideration of the material age evolution. *Heat Mass Transf.* **2017**, *54*, 1189–1197. [CrossRef]

53. Thoemen, H.; Irle, M.; Sernek, M. *Wood-Based Panels an Introduction for Specialists*; Brunel University Press: London, UK, 2010; ISBN 978-1-902316-82-6.

54. Ansell, M.P. (Ed.) 1—Wood microstructure—A cellular composite. In *Wood Composites*; Woodhead Publishing Ltd.: Cambridge, UK, 2015; pp. 3–26. [CrossRef]

55. Jiang, Y.; Lawrence, M.; Ansell, M.P.; Hussain, A. Cell wall microstructure, pore size distribution and absolute density of hemp shiv. *R. Soc. Open Sci.* **2018**, *5*, 171945. [CrossRef] [PubMed]